crystals

MDPI

Article

Two-Dimensional Electron Gas in Thin N-Polar GaN Channels on AlN on Sapphire Templates

Markus Pristovsek [1,*], Itsuki Furuhashi [1], Xu Yang [1], Chengzhi Zhang [2] and Matthew D. Smith [2]

[1] Center for Innovative Research of Future Electronics, Institute for Material Science and Systems for Sustainability, Nagoya University, Furo-cho, Chikusa-ku, Nagoya 464-8601, Japan; furuhashi.itsuki.r2@s.mail.nagoya-u.ac.jp (I.F.); yang.xu.y2@f.mail.nagoya-u.ac.jp (X.Y.)

[2] Center for Device Thermography and Reliability, School of Physics, University of Bristol, Tyndall Avenue, Bristol BS8 1TL, UK; chengzhi.zhang@bristol.ac.uk (C.Z.); matt.smith@bristol.ac.uk (M.D.S.)

* Correspondence: markus.pristovsek@nagoya-u.jp

Abstract: We report on 2-dimensional electron gases realized in binary N-polar GaN channels on AlN on sapphire templates grown by metal–organic vapor phase epitaxy. The measured sheet carrier density of 3.8×10^{13} cm^{-2} is very close to the theoretical value of 3.95×10^{13} cm^{-2} due to the low carbon and oxygen background doping in the N-polar GaN if grown with triethyl-gallium. By inserting an intermediate AlN transition layer, room temperature mobilities in 5 nm channels up to 100 cm^2/Vs were realized, probably limited by dislocations and oxygen background in N-polar AlN. Thicker channels of 8 nm or more showed relaxation and thus much lower mobilities.

Keywords: N-polar AlN; N-polar GaN; MOVPE; impurity incorporation; GaN relaxation

1. Introduction

Nitride-based high electron mobility transistors (HEMTs) have entered the mass market. Due to their exceptional performance at higher frequencies, any power RF-application using solid state devices has switched to GaN-based HEMTs. These are typically in the Ga-polar orientation where a 2-dimensional electron gas (2DEG) is generated at the interface between a GaN channel and an AlGaN barrier layer on top [1]. The performance of a HEMT strongly depends on the 2DEG. Higher sheet carrier densities in the 2DEG can be achieved by increasing the AlGaN content. However, this also increases the ohmic resistance to the channel without further measures. Moreover, AlGaN develops cracks for barrier layers thicker than 10 nm with an aluminum content of more than ≈60 %.

To further increase the switching speed, N-polar structures were developed [2]. When based on N-polar GaN, they have an AlGaN back barrier and a thin GaN channel on top. The thin GaN channel has good ohmic access, as it is directly on the surface, and is fast to deplete, as it is very thin. However, the AlGaN back barrier below limits the Al-content and, thus, the maximum carrier density in the 2DEG. Thus, the idea is to use N-polar AlN templates.

So far, N-polar HEMT development focused on high-frequency applications. However, N-polar AlN-based HEMTs are also interesting for power applications. Al-polar HEMTs that reach high breakdown voltages use AlGaN channels, which reduces mobility on templates with higher dislocation densities due to partially relaxed AlGaN buffer layers, e.g., [3]. Apart from reducing carrier mobilities, the partially relaxed AlGaN buffer layers also reduce the thermal conductivity. Finally, there is the top Al-rich AlGaN barrier in Al-polar HEMTs, which results in rather high contact resistances. N-polar AlN-based HEMTs have advantages for high voltage power with direct contact to the GaN channel, leading to low contact resistances and the lack of breakdown through the highly insulating AlN buffer, which has also a higher heat conductivity than GaN or AlGaN.

Citation: Pristovsek, M.; Furuhashi, I.; Yang, X.; Zhang, C.; Smith, M.D. Two-Dimensional Electron Gas in Thin N-Polar GaN Channels on AlN on Sapphire Templates. *Crystals* **2024**, *14*, 822. https://doi.org/10.3390/cryst14090822

Academic Editor: Nabeen K. Shrestha

Received: 20 August 2024
Revised: 31 August 2024
Accepted: 11 September 2024
Published: 20 September 2024

First, N-polar GaN/AlN HEMTs have been recently demonstrated on AlN bulk substrates by molecular beam epitaxy (MBE) [4,5]. For broader applications, growth on cheaper, large area substrates with the mainstream industrial technology of metal–organic vapor phase epitaxy (MOVPE) is desirable.

Unlike the growth of N-polar GaN by MOVPE, N-polar AlN layers on sapphire [6–10] or 4H-SiC [11,12] are typically quite rough (>3 nm) in the literature. In MBE, however, smooth N-polar AlN has been reported on (111) Si [13], SiC [14], and even bulk AlN [4]. MBE inherently has a much lower V/III ratio than MOVPE, and the recently achieved smooth N-polar AlN by MOVPE on sapphire also used very low V/III ratios [15,16]. Building on this, 2DEGs have been reported for AlGaN channel layers on AlN on vicinal sapphire by MOVPE [17] and HEMTs were demonstrated [17–21]. However, the alloy scattering inherent to the ternary AlGaN additionally limits the mobility, with the reported value ranging between 20 and 40 cm^2/Vs [17]. Just in print is a report with mobilities of up to 180 cm^2/Vs, suggesting that the dislocations in the AlN buffer are limiting the mobility [20]. Another recent work showed that, using tri-methylgallium as precursor at 650 °C, extremely high V/III ratios are needed to keep the carbon content low [21]. Thus, we chose to investigate N-polar GaN on AlN heterostructures on sapphire, focusing on the impurity incorporation and the interface to AlN.

2. Materials and Methods

The samples in this study were grown in a 3 × 2″ close coupled showerhead MOVPE reactor from EpiQuest with a fixed 18 mm gap. The total flow was 10 L/min. The susceptor temperatures were measured in situ, and were about 30–70 °C below the thermocouple temperatures. In the following, we will use the thermocouple temperatures, since the in situ system was not working during some of the growth experiments.

The substrates were (0001) sapphire 4° misoriented to [11$\bar{2}$0]. The growth of the N-polar AlN in this reactor has been reported before [16], and more details on the growth of N-polar GaN will be reported elsewhere. Essentially, a low V/III ratio is needed for smooth N-polar AlN, and low temperature (750–850 °C) are needed for smooth GaN channels. The precursors used were tri-methylalumium (TMAl), tri-methylgallium (TMGa) or tri-ethylgallium (TEGa), and ammonia (NH_3) with hydrogen as the carrier gas at a reactor pressure of 10 kPa and a total flow of 10 L, unless for the SIMS sample. For AlN, we used 0.8 Pa NH_3 and 0.47 Pa TMAl at 1280 °C set-point. The NH_3 was ramped during the transition layer to GaN to 5000 Pa, which is also used for GaN growth. The GaN channel was grown at 800 °C with a TEGa partial pressure of 0.52 Pa.

For secondary ion mass-spectrocopy (SIMS), we prepared a sample with five layers. At the bottom was the AlN buffer with a V/III ratio of 1.75. Then, the sample was cooled without growth to 1000 °C, and a GaN layer was grown at a V/III ratio of 1000 with 10 %NH_3 in the gas phase, followed by a GaN layer at 900 °C, both layers with TMGa. Then, the temperature was decreased to 850 °C, and the total flow was accidentally decreased to 6 L/min, leading to 80 % NH_3 in the gas phase. The V/III ratio was still 1000 for the growth of the last two layers at 850 °C, first with TMGa and then with TEGa. At the end of each layer, there was a short Si doping using monomethyl-silane (MMSi), which resulted also in a spike of the carbon content, either due to the change in the Fermi level or directly from the carbon from the MMSi.

The samples were characterized by tapping mode atomic force microscopy (AFM), X-ray reflectivity (XRR) for channel thickness, and X-ray diffraction (XRD) for structural characterization. Since GaN and AlN are relatively far in reciprocal space, we used the 10.5 reflection to characterize the strain state in reciprocal space maps because only for this reflection both GaN and AlN could be recorded in a single $\omega - 2\Theta$ reciprocal space map (RSM) with a an area detector in a five-axis diffractometer.

The sheet resistivity was mapped contactless via eddy currents. For detailed measurement, 10 × 10 mm pieces were cut from the 2″ templates and measured in a variable temperature Hall system with a 0.5 T magnet and the possibility for AC-hall measure-

ments, in case of low mobilities. Further measurements of the sheet resistance together with contact resistance was performed using circular transfer line measurements (cTLM). After cleaning by acetone/isopopanol/water, we spin-coated the lift-off resist (LOR7B) and photoresist (S1813) and developed for 20 s in a TMAH-based developer. After an oxygen plasma cleaning, the contact were deposited by electron beam evaporation, Ti/Al/Ni/Au (20/120/30/100 nm). Finally, the sample was annealed under nitrogen for 1 min at a range of temperatures before cTLM was measured.

3. Results and Discussion

We had established before the need for low V/III ratios for smooth N-polar AlN templates [16], and low growth temperature of GaN below 900 °C to avoid step-bunching, which otherwise develops at higher temperatures [22]. While simply growing a GaN layer on AlN delivered sheet carrier densities in the range of $2-3\times10^{13}$ cm^{-2}, the mobilities were very low, less than 3 cm^2/Vs. One suspect was carbon incorporation from the Ga precursor, tri-methylgallium.

We therefore performed a SIMS measurement, shown in Figure 1. We first focused on the N-polar AlN template. Comparing carbon and oxygen, the latter has a much higher concentration in the N-polar AlN. Furthermore, there are oscillation of the carbon and oxygen content at the beginning of the AlN layer. These are due to the spontaneous rotation of the bowed sapphire wafers in their pocket at high temperatures, as the SIMS central was cut a little off the center and which typically stopped after a certain AlN thickness has been grown. The difference in the impurity incorporation is caused by a temperature gradient from the inside to the outside of the susceptor because the outer heater reaches 100% power already at 1200 °C. Therefore, the outer area is about 30–50 °C colder at 1280 °C setpoint, leading to a higher carbon incorporation at the outer edge and an oscillation when a wafer rotates in its pocket.

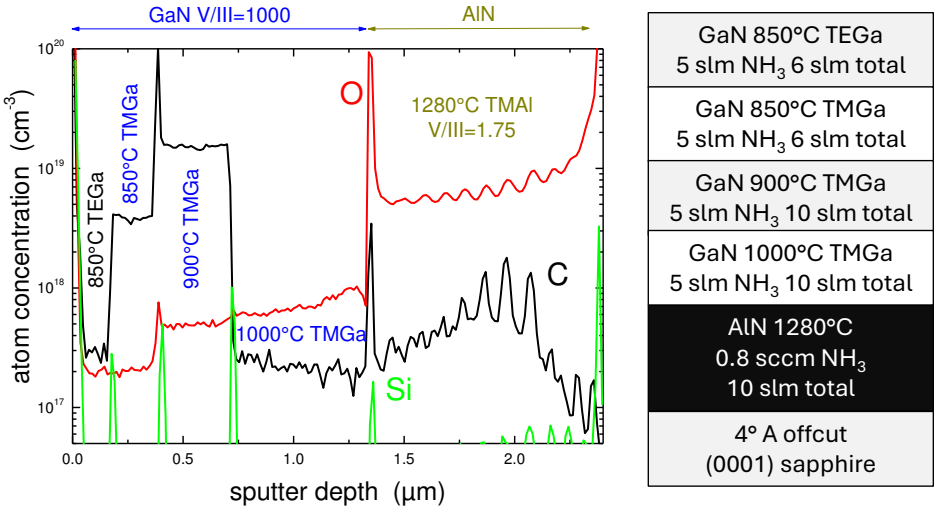

Figure 1. SIMS measurement of an N-polar AlN with four different GaN layers on top. Right: a sketch of the layer stack.

Looking at the stabilized levels, the oxygen level is much higher in the range of mid-to-high 10^{18} cm^{-3}, while carbon is ten times less, despite the very low V/III ratio close to unity. A much higher oxygen concentration in N-polar AlN, even in the $\approx 5\times10^{19}$ cm^{-3} range compared to 1×10^{19} cm^{-3} on Al-polar AlN, has been also reported by Takeuchi et al. [6], and recently by Kowaki et al. in Figure 5 of [20]. The high oxygen incorporation in N-polar AlN has two main reasons.

First, N-polar AlN must be grown under very Al-rich conditions. The NH_3 flow rate is so low that the AlN start to desorb and the growth rate is already decreasing [16]. N-polar GaN also shows a very high oxygen incorporation at Ga-rich conditions [23,24], which had

been predicted for a Ga-covered N-polar GaN by theory before [25]. At similar metal-rich conditions, the N-polar surface, with its single metal layer, picks up more oxygen than the double metal layer Al-rich surface of Al-polar AlN, which is present under the most Al-rich conditions [26]. A new calculation suggests that the high offcut used for N-polar growth also increases the incorporation of oxygen [27]. For N-polar GaN, increasing the V/III rate to above 1000 resulted in much lower oxygen incorporation [23,24]. Growing N-polar AlN with a high V/III ratio is very challenging, and usually results in a rough surface as discussed in the introduction.

The second reason for a high oxygen background in AlN is the relatively low growth rate of AlN, at 460 nm/h or less. This slow growth rate is necessary to obtain a smooth surface [16], but gives more oxygen a chance to incorporate. This is even more severe during the growth interruption due to lowering the temperature at the end of the AlN growth. During the 7 min, the exposed AlN surface accumulated a very high oxygen concentration, leading to a high oxygen peak at the AlN/GaN interface in Figure 1. Even though the role of oxygen in AlN is still not fully clarified, such a high oxygen impurity concentration at the interface is certainly not good for the mobility of the 2DEG.

Therefore, we tried to shorten the growth interruption from N-polar AlN to the start of the GaN channel growth. To further reduce the O content in AlN, we introduced an intermediate AlN layer with a higher V/III ratio while ramping the temperature. Therefore, we increased the NH_3 flow during AlN growth to the 50% maximum, resulting in a V/III ratio of 5500 while decreasing the temperature to 1100 °C. To shorten the time that the AlN was exposed, after 4 minutes (less than 10 nm of AlN growth at this high V/III ratio), we decreased the temperature to 950 °C in 90 s while still growing AlN. Then, TMAl was switched to the vent and the heater was set (not ramped) to 875 °C. As Figure 2 shows, the buffer has a very nice regular step-bunching with an RMS roughness of 0.3 nm. The surface after growing the intermediate layer was more irregular, but generally smooth with almost the same RMS roughness (excluding the dots). The dots in the right AFM image were due to a too long nitridation time of that sample, and were also found on samples without an intermediate layer.

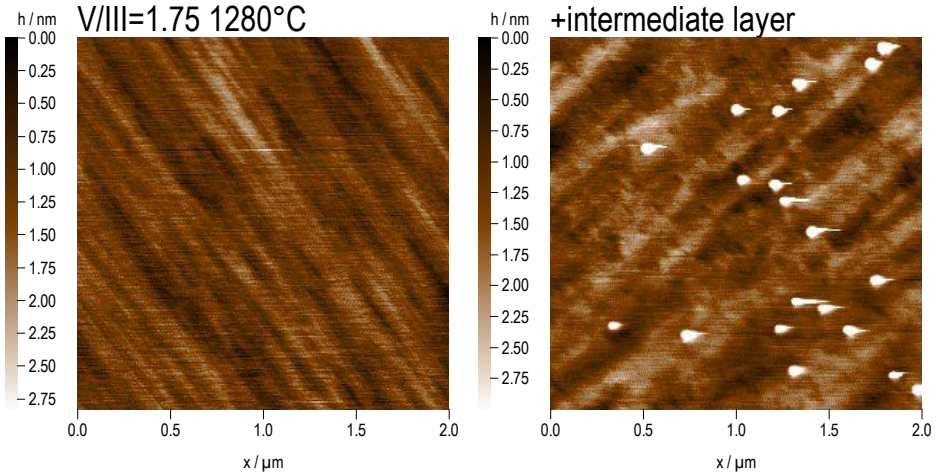

Figure 2. Surfaces of AlN after buffer with a V/III ratio of 1.75, with an additional intermediate layer with high V/III ratio, and growing while ramping the temperature down. The small dots are from defects from a too long/too hot nitridation prior to the AlN growth.

Using this procedure, we could reduce the growth interruption between AlN and GaN from 7 min to 75 s. After 75 s, we started growing the GaN channel using TEGa for 2 min (5–6 nm GaN) while ramping the heater to 850 °C which resulted in a growth temperature of (850 ± 25) °C for the GaN channel and smooth surface (apart from the dots) as seen in the inset in Figure 3.

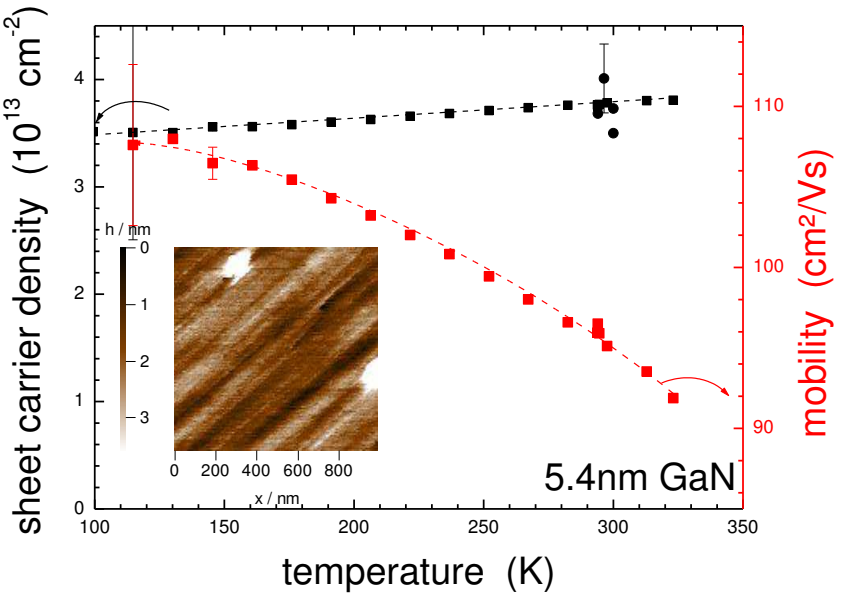

Figure 3. Variable temperature Hall measurement of sheet carrier concentration (left axis, black circles) and mobility (right axis, red squares) for an optimized sample with a channel thickness of 5.4 nm. The circle are sheet carrier measurements of samples with lower mobility. The inset shows the GaN surface of that sample.

Apart from oxygen in AlN, the carbon content in GaN is also important, because carbon forms a deep level and thus reduces the carrier mobility. For N-polar GaN, lower carbon incorporation was reported at high temperatures compared to Ga-polar [23,24,28], while at lower temperatures, the ratio was inverted [28]. The V/III ratio had little impact on the carbon, no matter the growth temperature [23,24,28]. This is very different from Ga-polar GaN, where the oxygen is low but the carbon depends strongly on the V/III ratio. Only at the very low growth temperature of 650 °C, a strong correlation of carbon content and V/III ratio from mid 10^{17} cm^{-3} at V/III = 45,000 to upper 10^{19} cm^{-3} at V/III = 15,000 has been reported [21].

Figure 4 compares the carbon incorporation in our N-polar GaN to the one into Ga-polar GaN from the literature. Since the carbon incorporation depends strongly on the V/III ratio in Ga-polar GaN, we selected literature data with a comparable carbon concentration at 1000 °C, which were the data from Koleske et al. [29] (V/III = 1000), Danielsson et al. [30] (V/III = 625), and Loeto et al. [31] (no V/III ratio given). The slope of the Ga-polar samples is close to the slope of our N-polar GaN. However, below 900 °C, the carbon content even decreases (but this may be due to an accidentally higher NH_3 partial pressure) while the carbon content in Ga-polar increases. Still, almost 50× less carbon is incorporated at 850 °C in N-polar GaN. When switching to TEGa for GaN growth, the carbon reduces to 3×10^{17} cm^{-3}, almost the same carbon level as for the GaN grown at 1000 °C with TMGa.

Finally, the oxygen content in the N-polar GaN in Figure 1 was at all temperatures is between $2 - 5 \times 10^{17}$ cm^{-3}, a factor of 10 lower than recently reported values for N-polar GaN grown at 800 °C and 650 °C with TMGa of low-to-mid 10^{18} cm^{-3} [21]. Thus, the low oxygen background and the comparable low carbon background doping would not limit the GaN channel mobility when using TEGa, even for growth at 850 °C.

As Figure 3 shows, the carrier concentration is almost temperature independent. The sheet carrier concentration linearly reduces from 3.78×10^{13} cm^{-2} at 300 K to 3.49×10^{13} cm^{-2} at 100 K. The linear reduction suggests that this is rather due to thermal expansion and the temperature-dependent changes in the band gap, the elastic, and the piezoelectric coefficients, and not due to the freezing out of carriers. Moreover, the 3×10^{17} cm^{-3} oxygen background in GaN, according to the SIMS data from Figure 1, translates to only 1.62×10^{11} cm^{-2} sheet carrier density, which is much less than observed

change. The expected sheet carrier concentration from the piezo- and pyro-polarization induce charge for GaN strained on AlN would be 3.95×10^{13} cm^{-2} following [1] with updated elastic and piezo-electric tensors, which again indicates that there were very few deep traps and no background doping in our GaN channel layers.

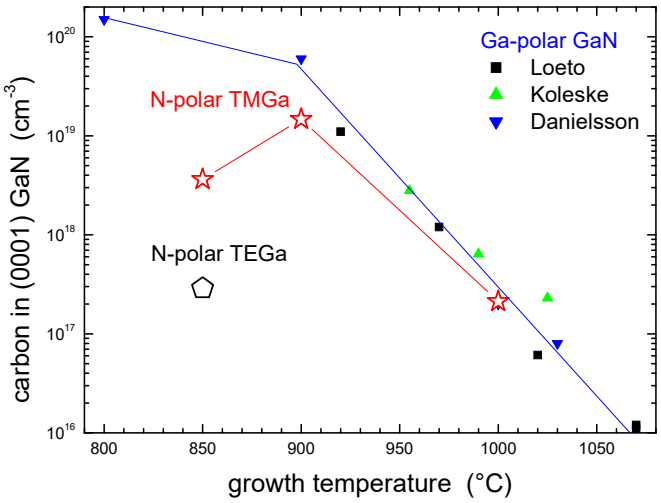

Figure 4. Carbon concentration in N-polar GaN (our data, Figure 1) and Ga-polar GaN from the literature [29–31].

We observed the onset of relaxation (≈10 %) for one 7.4 nm thick N-polar GaN layer on AlN while a 7.2 nm film was fully strained (see Figure 5). Since both the templates were slightly different quality, about 8 nm is the thickness limit for a coherent GaN channel on AlN for our current set of growth conditions. A recent paper demonstrated the coherent growth of 9.5 nm of N-polar GaN on AlN while an 11 nm thick GaN layer on Al-polar AlN was 70 % relaxed [21]. Furthermore, also MBE reported no relaxation on N-polar bulk AlN for thicknesses up to 10 nm [5]. Hence, with different growth conditions (e.g., a lower GaN growth temperature), a critical thickness of 10 nm seems possible for MOVPE for N-polar GaN on AlN.

Compared to the strong change in relaxation, the roughness did not change much with GaN thickness. Only above 10 nm did the step-bunching become more severe (Figure 5, right), while the relaxation increased from almost zero to 35 %. Thus, it is not surprising that the mobility shows a much stronger correlation with relaxation than with the RMS roughness (Figure 6a).

This raises the question, what is limiting the 2DEG mobility? A previous study on N-polar GaN channels has calculated the impact of several effects and showed that, for thin channels, the roughness scattering at surfaces and interfaces dominates [32]. There was also an increase in mobility reported for GaN channels on top of N-polar AlN substrates (with an $Al_{0.91}Ga_{0.09}N$ interlayer) when the layer thickness increased from 5 to 8 nm [4] (plotted in Figure 6b). In comparison, our mobilities stayed the same or slightly reduced with increasing thickness from 5.5 nm to 7.2 nm (Figure 6b). This indicates that scattering mechanisms other than interface roughness are dominating, which explains the relatively low mobilities. And, indeed, when plotting the roughness versus the mobility, there is no correlation in Figure 6. However, when plotting the strain relaxation versus the mobility, a clear correlation is seen in Figure 6a. Thus, misfit dislocations reduce the mobility. Therefore, dislocation in the AlN should also strongly limit the mobility.

Indeed, the mobility went up to a certain extent with thicker AlN buffer layers, which have a narrower FHWM of the 10.2 reflection in XRD, as shown in Figure 7. However, a 2 h AlN template did not follow the trend which was probably due to a strong step-bunching developing on that sample which reduced the effective channel width. The general trend of

the 30 and 60 min samples agrees with the data of [20] and points that at the moment our mobility is limited by the dislocations in the N-polar AlN buffer, which was also suggested by Kowaki et al. [20].

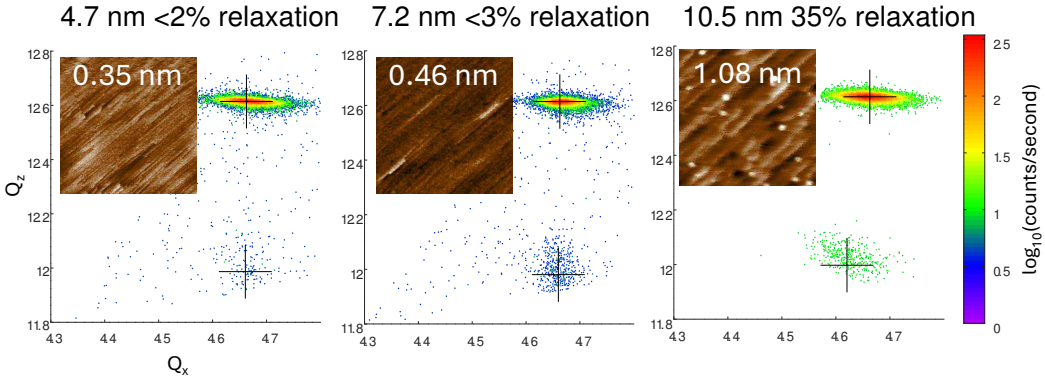

Figure 5. RSM of the 10.5 reflection and (1 × 1) μm^2 AFM images with RMS roughness for three different GaN channel thicknesses on N-polar AlN. The color bar is the logarithm of the counts.

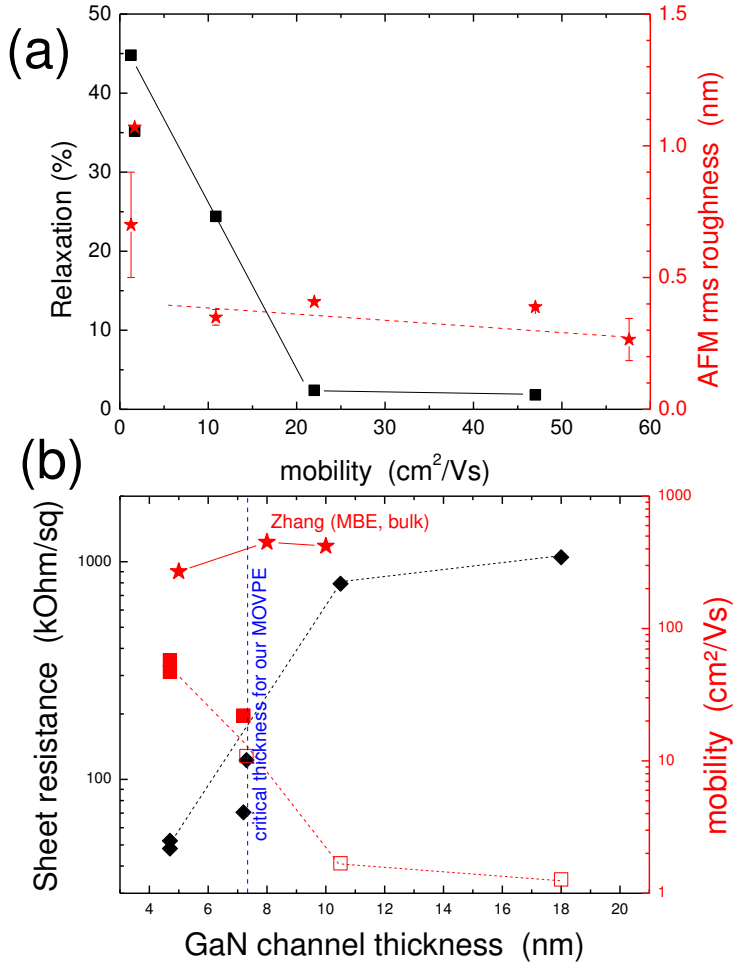

Figure 6. (**a**) Strain relaxation (left axis, black squares) and RMS roughness (right axis, red stars) plotted versus the mobility. (**b**) Sheet resistance (left axis, black squares) and mobility (right axis, red suqares (our, red stars) [4] for different thicknesses with simple intermediate AlN layer (open symbols calculated from contactless sheet resistance).

To obtain an idea of the current threading dislocation (TD) density in our N-polar AlN templates, we counted the density of small hillocks when overgrowing an AlN template

with AlN intermediate V/III ratios (50–200). Using a 30 min template gave a density of 5×10^9 cm^{-2}, which decreased to $2-3 \times 10^9$ cm^{-2} on a 60 min template. These are reasonable numbers for the TD density in N-polar AlN, as for rough N-polar AlN Takeuchi et al. reported a TD density of $\approx 10^{10}$ cm^{-2} [6]. If overgrown with AlN using even higher V/III ratios (around 2000), we found a density of hexagonal hillocks of $2-4 \times 10^8$ cm^{-2}, which is probably the density of c- and mixed-type TDs.

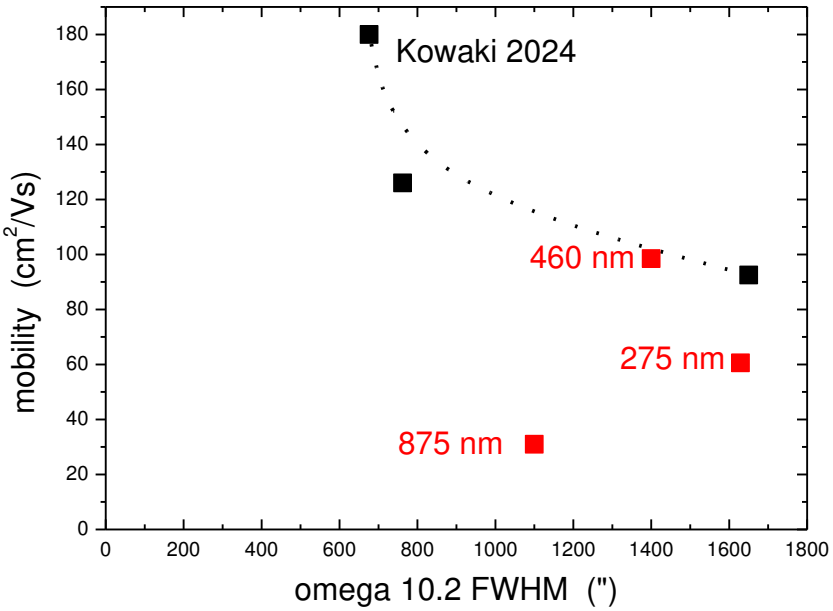

Figure 7. XRD rocking curve width of the skewsymmetric 10.2 reflection of the AlN buffer layer and the mobility of 5.5 nm thick GaN channels. Black data from [20], red our data after 30 min, 60 min and 120 min of AlN buffer layer growth, resulting in the indicated thicknesses.

Thus, oxygen related traps at the AlN/GaN interface and dislocations are the limiting the mobility in our samples. The difference of the templates is our main suspect as to why, at 5 nm channel width, our mobilities were still a factor of 2–3 or more below the reported ones in refs. [4,20,32], and do not increase when increasing the GaN channel layer thickness. The roughness is not the limit right now, and relaxation is not an issue for layers thinner than 8 nm.

Since our best channels were 5.5 nm thin, we wanted to see whether low-resistance ohmic contacts could be formed to them. For this, we processed a 5.4 nm GaN channel sample with a mobility of 96 cm^2/Vs with cTLM using Ti/Al/Ni/Au contacts as described in the experimental section. In the literature, annealing of Ti/Al/Ti/Au contacts to N-polar AlGaN channels used 850 °C (at 30 s) [19]. However, we worried about the stability of the very thin GaN channels, and thus tested several temperatures.

The contact resistance decreased upon annealing as can be seen in Figure 8. However, when annealing at temperatures above 500 °C, the sheet resistance increased as the 5.4 nm GaN under the contact was gradually eaten up by alloying, and was completely gone at 800 °C. Thus, contact resistance at 500 °C is $(115 \pm 65) \times 10^{-6}$ Ωcm^2, which is quite similar to the value of 94×10^{-6} Ωcm^2 for the recently published cTLM data of Ge-doped GaN [33]. However, using a roughened n+ Si-doped GaN regrowth of 27 nm, specific contact resistances of 0.17×10^{-6} Ωcm^2 have been reported using as-deposited Ti/Au contacts on semi-insulating N-polar GaN templates [34]. While such a thick GaN layer would relax during regrowth on AlN, thinner n+ Si:GaN layers with Ti/Au contacts have been also used in MBE for GaN channels on N-polar AlN and gave a contact resistance of 13×10^{-6} Ωcm^2 [5] (calculated from the TLM data). So while our contacts work even to ultra-thin GaN channels, there is certainly room for improvement.

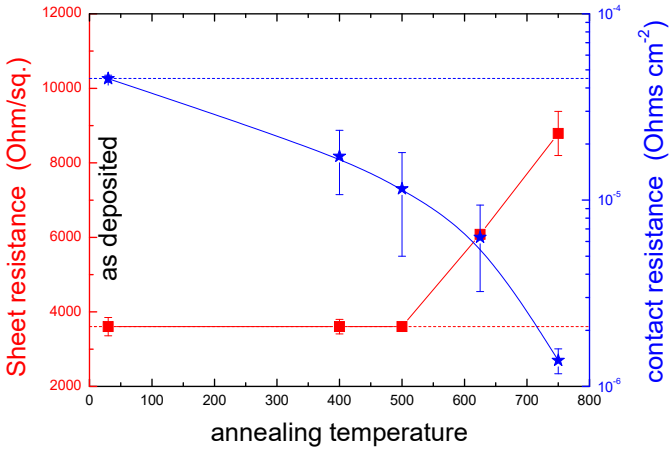

Figure 8. Specific contact resistance (left axis, red squares) and sheet resistance (right axis, blue stars) for contacts annealed at different temperatures.

4. Conclusions

We have demonstrated 2DEGs at a binary AlN/GaN hetero-junction on N-polar AlN grown on sapphire. The AlN and GaN show a relatively low oxygen background, and using TEGa as precursor, low carbon even for GaN channel growth at 800 °C. The carrier mobilities in 5.5 nm GaN channels were close to 100 cm^2/Vs, and are currently limited by the dislocation density of the AlN templates, and probably also by the oxygen traps in N-polar AlN near the AlN/GaN interface. We could form ohmic contact to 5 nm GaN channels and the contact resistance improved by annealing below 600 °C without affecting the GaN channel sheet resistance.

Author Contributions: Conceptualization, M.P. and I.F.; Data curation, M.P., I.F., X.Y., C.Z. and M.D.S.; Investigation, M.P., I.F., X.Y., C.Z. and M.D.S.; Writing—original draft, M.P.; Writing—review & editing, M.P. and I.F. All authors have read and agreed to the published version of the manuscript.

Funding: This research received no external funding.

Data Availability Statement: The data presented in this study are available on request from the corresponding author. The data are not publicly available due to some of it being in a proprietary format and needing a special software.

Conflicts of Interest: The authors declare no conflicts of interest.

Abbreviations

The following abbreviations are used in this manuscript:

RMS	root mean square
XRD	X-Ray Diffraction
FWHM	Full Width at Half Maximum
AFM	Atomic Force Microscopy
SIMS	Secondary Ion Mass Spectroscopy
2DEG	two-dimensional electron gas
TD	threading dislocation
cTLM	circular transfer line measurement

References

1. Ambacher, O.; Smart, J.; Shealy, J.R.; Weimann, N.G.; Chu, K.; Murphy, M.; Schaff, W.J.; Eastman, L.F.; Dimitrov, R.; Wittmer, L.; et al. Two-dimensional electron gases induced by spontaneous and piezoelectric polarization charges in N- and Ga-face AlGaN/GaN heterostructures. *J. Appl. Phys.* **1999**, *85*, 3222–3233. [CrossRef]
2. Wong, M.H.; Keller, S.; Nidhi, S.D.; Denninghoff, D.J.; Kolluri, S.; Brown, D.F.; Lu, J.; Fichtenbaum, N.A.; Ahmadi, E.; Singisetti, U.; et al. N-polar GaN epitaxy and high electron mobility transistors. *Semicond. Sci. Technol.* **2013**, *28*, 074009. [CrossRef]
3. Wu, Y.; Zhang, J.; Zhao, S.; Zhang, W.; Zhang, Y.; Duan, X.; Chen, J.; Hao, Y. More Than 3000 V Reverse Blocking Schottky-Drain AlGaN-Channel HEMTs with >230 MW/cm^2 Power Figure-of-Merit. *IEEE Electron Device Lett.* **2019**, *40*, 1724–1727. [CrossRef]
4. Zhang, Z.; Encomendero, J.; Kim, E.; Singhal, J.; Cho, Y.; Nomoto, K.; Toita, M.; Xing, H.G.; Jena, D. High-density polarization-induced 2D electron gases in N-polar pseudomorphic undoped GaN/Al0.85Ga0.15N heterostructures on single-crystal AlN substrates. *Appl. Phys. Lett.* **2022**, *121*, 082107. [CrossRef]
5. Kim, E.; Zhang, Z.; Encomendero, J.; Singhal, J.; Nomoto, K.; Hickman, A.; Wang, C.; Fay, P.; Toita, M.; Jena, D.; et al. N-polar GaN/AlGaN/AlN high electron mobility transistors on single-crystal bulk AlN substrates. *Appl. Phys. Lett.* **2023**, *122*, 092104. [CrossRef]
6. Takeuchi, M.; Shimizu, H.; Kajitani, R.; Kawasaki, K.; Kinoshita, T.; Takada, K.; Murakami, H.; Kumagai, Y.; Koukitu, A.; Koyama, T.; et al. Al- and N-polar AlN layers grown on c-plane sapphire substrates by modified flow-modulation MOCVD. *J. Cryst. Growth* **2007**, *305*, 360–365. [CrossRef]
7. Kirste, R.; Mita, S.; Hussey, L.; Hoffmann, M.P.; Guo, W.; Bryan, I.; Bryan, Z.; Tweedie, J.; Xie, J.; Gerhold, M.; et al. Polarity control and growth of lateral polarity structures in AlN. *Appl. Phys. Lett.* **2013**, *102*, 181913. [CrossRef]
8. Hussey, L.; White, R.M.; Kirste, R.; Mita, S.; Bryan, I.; Guo, W.; Osterman, K.; Haidet, B.; Bryan, Z.; Bobea, M.; et al. Sapphire decomposition and inversion domains in N-polar aluminum nitride. *Appl. Phys. Lett.* **2014**, *104*, 032104. [CrossRef]
9. Zhang, J.; Zhang, X.; Fan, A.; Chen, S.; He, J.; Nasir, A.; Zhuang, Z.; Lyu, J.; Hu, G.; Cui, Y. Achievement of polarity reversion from Al(Ga)-polar to N-polar for AlGaN film on AlN seeding layer grown by a novel flow-modulation technology. *J. Mat. Sci. Mat. Electron.* **2021**, *32*, 7858–7866. [CrossRef]
10. Xu, S.; Zhang, X.; Luo, X.; Fang, R.; Lyu, J.; Lai, M.J.; Hu, G. Improvements in characteristics of N-polar Si-doped AlGaN epi-layer grown on mis-oriented c-plane sapphire substrate. *Mater. Sci. Semicond. Process.* **2023**, *160*, 107447. [CrossRef]
11. Lemettinen, J.; Okumura, H.; Kim, I.; Rudzinski, M.; Grzonka, J.; Palacios, T.; Suihkonen, S. MOVPE growth of nitrogen- and aluminum-polar AlN on 4H-SiC. *J. Cryst. Growth* **2018**, *487*, 50–56. [CrossRef]
12. Zhang, H. Hot-wall MOCVD of N-Polar Group-III Nitride Materials and High Electron Mobility Transistor Structures. Ph.D. Thesis, Linköping University Electronic Press, Linköping, Sweden, 2022. [CrossRef]
13. Dasgupta, S.; Wu, F.; Speck, J.S.; Mishra, U.K. Growth of high quality N-polar AlN $(000\bar{1})$ on Si (111) by plasma assisted molecular beam epitaxy. *Appl. Phys. Lett.* **2009**, *94*, 151906. [CrossRef]
14. Hu, M.; Wang, P.; Wang, D.; Wu, Y.; Mondal, S.; Wang, D.; Ahmadi, E.; Ma, T.; Mi, Z. Heteroepitaxy of N-polar AlN on C-face 4H-SiC: Structural and optical properties. *APL Mater.* **2023**, *11*, 121111. [CrossRef]
15. Isono, T.; Ito, T.; Sakamoto, R.; Yao, Y.; Ishikawa, Y.; Okada, N.; Tadatomo, K. Growth of N-Polar Aluminum Nitride on Vicinal Sapphire Substrates and Aluminum Nitride Bulk Substrates. *Phys. Stat. Solidi (b)* **2020**, *257*, 1900588. [CrossRef]
16. Pampili, P.; Pristovsek, M. Nitrogen-polar growth of AlN on vicinal (0001) sapphire by MOVPE. *J. Appl. Phys.* **2024**, *135*, 195303. [CrossRef]
17. Miyamoto, M.; Matsumura, W.; Okuno, R.; Matsuda, S.; Hanasaku, K.; Kowaki, T.; Inahara, D.; Kurai, S.; Okada, N.; Yamada, Y. Improvement of electrical properties by insertion of AlGaN interlayer for N-polar AlGaN/AlN structures on sapphire substrates. *Jpn. J. Appl. Phys.* **2023**, *62*, SN1016. [CrossRef]
18. You, L.; Matsumura, W.; Ataka, K.; Matsuda, S.; Inahara, D.; Hanasaku, K.; Okuno, R.; Kowaki, T.; Yao, Y.; Ishikawa, Y.; et al. Growth and characterization of nitrogen-polar AlGaN/AlN and demonstration of field effect transistor. *Jpn. J. Appl. Phys.* **2022**, *62*, SA1018. [CrossRef]
19. Inahara, D.; Matsuda, S.; Matsumura, W.; Okuno, R.; Hanasaku, K.; Kowaki, T.; Miyamoto, M.; Yao, Y.; Ishikawa, Y.; Tanaka, A.; et al. Investigation of Electrical Properties of N-Polar AlGaN/AlN Heterostructure Field-Effect Transistors. *Phys. Stat. Solidi (a)* **2023**, *220*, 2200871. [CrossRef]
20. Kowaki, T.; Hanasaku, K.; Miyamoto, M.; Zazuli, A.H.; Inahara, D.; Fujii, K.; Kimoto, T.; Ninoki, R.; Kurai, S.; Okada, N.; et al. Effect of the Twist Crystallinity of N-Polar AlN Underlayer on the Electrical Properties of GaN/AlN Structures. *Phys. Status Solidi (a)* **2024**, 2400053, *early view*. [CrossRef]
21. Zazuli, A.H.; Kowaki, T.; Miyamoto, M.; Hanasaku, K.; Inahara, D.; Fujii, K.; Kurai, S.; Okada, N.; Yamada, Y. Electrical Properties of N-Polar GaN/AlGaN/AlN Grown via Metal-Organic Vapor Phase Epitaxy. *Phys. Status Solidi (a)* **2024**, 2400060, *early view*. [CrossRef]
22. Furuhashi, I.; Pristovsek, M.; Yang, X. N-polar GaN/AlN heterostructures on sapphire grown by metal-organic vapor phase epitaxy. *J. Cryst. Growth to be submitted*.
23. Pristovsek, M.; Furuhashi, I.; Pampili, P. Growth of N-Polar $(000\bar{1})$ GaN in Metal–Organic Vapour Phase Epitaxy on Sapphire. *Crystals* **2023**, *13*, 1072. [CrossRef]
24. Fichtenbaum, N.; Mates, T.; Keller, S.; DenBaars, S.; Mishra, U. Impurity incorporation in heteroepitaxial N-face and Ga-face GaN films grown by metalorganic chemical vapor deposition. *J. Cryst. Growth* **2008**, *310*, 1124–1131. [CrossRef]

25. Sun, Q.; Selloni, A.; Myers, T.H.; Doolittle, W.A. Oxygen adsorption and incorporation at irradiated GaN(0001) and GaN(000$\bar{1}$) surfaces: First-principles density-functional calculations. *Phys. Rev. B* **2006**, *74*, 195317. [CrossRef]
26. Pristovsek, M.; Bellman, K.; Mehnke, F.; Stellmach, J.; Wernicke, T.; Kneissl, M. Surface transitions of (0001) AlN during metal-organic vapour phase epitaxy. *Phys. Stat. Sol. (a)* **2017**, *254*, 1600711. [CrossRef]
27. Akiyama, T.; Kawamura, T. An Ab Initio Study for Oxygen Adsorption Behavior on Polar GaN Surfaces. *Phys. Stat. Sol. (b)* **2024**, 2300573, *early view*. [CrossRef]
28. Cruz, S.C.; Keller, S.; Mates, T.E.; Mishra, U.K.; DenBaars, S.P. Crystallographic orientation dependence of dopant and impurity incorporation in GaN films grown by metalorganic chemical vapor deposition. *J. Cryst. Growth* **2009**, *311*, 3817–3823. [CrossRef]
29. Koleske, D.; Wickenden, A.; Henry, R.; Twigg, M. Influence of MOVPE growth conditions on carbon and silicon concentrations in GaN. *J. Cryst. Growth* **2002**, *242*, 55–69. [CrossRef]
30. Danielsson, Ö.; Li, X.; Ojamäe, L.; Janzén, E.; Pedersen, H.; Forsberg, U. A model for carbon incorporation from trimethyl gallium in chemical vapor deposition of gallium nitride. *J. Mater. Chem. C* **2016**, *4*, 863–871. [CrossRef]
31. Loeto, K.; Kusch, G.; Ghosh, S.; Kappers, M.; Oliver, R. Quantitative analysis of carbon impurity concentrations in GaN epilayers by cathodoluminescence. *Micron* **2023**, *172*, 103489. [CrossRef]
32. Singisetti, U.; Hoi Wong, M.; Mishra, U.K. Interface roughness scattering in ultra-thin N-polar GaN quantum well channels. *Appl. Phys. Lett.* **2012**, *101*, 012101. [CrossRef]
33. Yamada, S.; Shirai, M.; Kobayashi, H.; Arai, M.; Kachi, T.; Suda, J. Realization of low specific-contact-resistance on N-polar GaN surfaces using heavily-Ge-doped n-type GaN films deposited by low-temperature reactive sputtering technique. *Appl. Phys. Express* **2024**, *17*, 036501. [CrossRef]
34. Hatui, N.; Krishna, A.; Li, H.; Gupta, C.; Romanczyk, B.; Acker-James, D.; Ahmadi, E.; Keller, S.; Mishra, U.K. Ultra-high silicon doped N-polar GaN contact layers grown by metal-organic chemical vapor deposition. *Semicond. Sci. Technol.* **2020**, *35*, 095002. [CrossRef]